# GSA Data Repository 2016257

Shock-metamorphosed rutile grains containing the high-pressure polymorph

$TiO_2$-II in four Neoarchean spherule layers

Frank C. Smith, Billy P. Glass, Bruce M. Simonson, Joseph P. Smith, Alexandra E. Krull-Davatzes, and Karl S. Booksh

correspondence to: fcsmith@udel.edu

**This PDF file includes:**

**Methods**

Samples. Simonson and colleagues collected all the hand samples from surface outcrops or from float directly in front of an outcrop. Carawine spherule layer (CSL) samples X24-1, 43-1, 42-1A, and X38-2, Carawine context sample 104175, Bee Gorge samples 96714A & B, Monteville spherule layer (MSL) sample U63-1, and Monteville context sample T149-1 were partially sawn or sawn into slabs at Oberlin College. MSL sample U63-1 had some oil contamination from the rock saw at Oberlin College. F. C. Smith photographed, described, and prepared the samples.

Steps taken to minimize sample contamination. The trim saw table and blade were brushed and washed before and after a sample was sawn. Metal tongs, glass beakers, glass stirring rods, stirring magnets, and glass separatory funnels were washed with soap and warm water, dried, and rinsed with Fisher Scientific (Fair Lawn, New Jersey) acetone (Certified ACS). The heavy liquid (see below) was filtered before it was poured into a separatory funnel, and it was usually filtered again before it was returned to the bottle. The separatory funnels were cleaned between separations involving different samples, layers/sublayers within a sample, subsamples, and size fractions. A glass syringe used during heavy liquid separation was often rinsed with acetone. After heavy liquid separation, filters containing sample material were kept closed and covered with plastic wrap during storage.

The steel mortar and pestle used for sample crushing was cleaned with acetone before and after use. We used W. S. Tyler standard 3-inch brass sieves for wet and dry sieving. Prior to use, a sieve was cleaned using water and ultrasonic agitation, and the mesh was examined for grains and/or damage using a binocular microscope with up to 50× magnification. Beakers containing sample material were covered with plastic wrap, except when they were in the oven. Boxes containing supplies, e.g., filters, weighing paper, and vials, were kept closed. Small

brushes were cleaned using water and ultrasonic agitation, dried, and examined for contaminant grains using a binocular microscope.

Contaminant particles. Sample contamination appears to be minor and limited to small plastic particles, fibers, malachite and solder particles from the laboratory water pipes, and rust particles that are most likely from the separatory funnel stands and possibly the fume hoods. In MSL sample U63-1, ~75 blue and green heavy mineral grains, mostly in the 63-125 μm size fraction, were identified as silicon carbide using micro-Raman spectroscopy. We interpret these grains as contaminant particles from the rock saw or sandpaper at Oberlin College.

Trimming, sawing, cleaning, and drying the samples. At the University of Delaware, weathered parts of the samples were trimmed off and the samples were sawn into pieces using a water-cooled trim saw with a diamond-tipped blade. For Bee Gorge sample BB which consists of the Bee Gorge spherule layer (BGSL) sandwiched between two context layers (Table DR2), the two context layers were each sawn from the BGSL, and the three layers were processed separately. Bee Gorge samples 96714A & B (Table DR2; Fig. DR1) are mirror-image slabs from the same hand sample that encompass the same stratigraphic interval. For both samples, the basal carbonate lutite (Bcl) context layer was sawn from the BGSL, and the BGSL was sawn into three stratigraphic subdivisions: lowermost spherule-rich sublayer (Lspsl), spherule-bearing lutite sublayer (Splsl), and the upper spherule/lutite sublayers (Usplsl). For both samples, the Bcl context layer and the three subdivisions of the BGSL were each processed separately.

If necessary, a sample was sawn into two or more pieces such that each piece would easily fit in a 1 L glass beaker for acid digestion (see below). The pieces were rinsed with tap and/or distilled water, and for about two-thirds of the samples, the pieces were quickly immersed in HCl or $HNO_3$ (see below) and then rinsed again. For about half of the samples, the pieces

were immersed in glass beakers filled with tap or distilled water, and they underwent ultrasonic agitation for several minutes. After a final rinsing with tap or distilled water, the pieces were placed in a glass beaker, and the beaker was put in an oven for at least 12 hours at a temperature (T) of ~60-70 °C.

Sample weights. The larger pieces (>100 g) were weighed on an Ohaus Triple Beam balance with a readability of 0.1 g. Most of the smaller pieces (<100 g) were weighed on a Sartorius 1801 MP8 electronic analytical balance with a readability of 0.1 mg. For Bee Gorge samples BB, 96714A, and 96714B, each of the layers and sublayers was weighed separately (Table DR 6). Most of the samples, layers, and sublayers consisted of two or more subsamples, e.g., Carawine context sample X68-1 (604.7 g; Table DR4) consisted of subsamples 300.0 g and 304.7 g. In Tables DR4-DR7, weights are reported to one or two decimal places. The weight of a sample weighed on the Triple Beam balance is reported to one decimal place. The weight of a sample, layer, or sublayer(s) weighed on the analytical balance is reported to two decimal places in order to be conservative, since sometimes the balance would not stabilize in the third or fourth decimal place.

Boiling and crushing of samples. For Jeerinah spherule layer (JSL) sample W94-1Q, MSL sample V111, and the basal carbonate lutite (Bcl) layers in Bee Gorge samples 96714A & B, some or all of the subsamples were boiled for one to four days in either a saturated solution of Fisher Scientific sodium pyrophosphate ($Na_4P_2O_7 \cdot 10H_2O$) (Certified ACS) or water in order to break up the clay-sized material. JSL samples W94-1Q and X21-1 did not react with room temperature HCl, and they were crushed so that most of the material would pass through a 250 µm sieve. For Bee Gorge sample BB, the BGSL and the two context layers were each slightly crushed prior to acid digestion (see below). For Bee Gorge samples 96714A & B (Table DR2;

Fig. DR1), the basal carbonate lutite (Bcl) material was slightly crushed and put through acid digestion (see below), and the acid-insoluble residues were crushed below 125 μm. For sample 96714A, the spherule-bearing lutite sublayer (Splsl) was slightly crushed before acid digestion, and the acid-insoluble residue was crushed below 125 μm before the spherules were handpicked from the >250 μm size fraction. For sample 96714A, the acid-insoluble material in the >250 μm size fractions of the two subsamples that comprise the lowermost spherule-rich sublayer (Lspsl) was slightly crushed, and after the spherules and spherule fragments were handpicked from this material, the remaining material was crushed below 125 μm. Each of the remaining six subsamples of the BGSL in samples 96714A & B was crushed below 125 μm after the spherules had been handpicked from the acid-insoluble material in the >250 μm size fractions. Millimeter-sized and smaller acid-resistant grains in subsample 304.7 g of Carawine context sample X68-1 and Bee Gorge context sample 92058 were crushed below 250 μm.

Acid digestion. All the samples went through warm acid baths using one or more of the following acids: Fisher Scientific concentrated (12.1 N) HCl (Certified ACS Plus), Fisher Scientific concentrated (15.8 N) $HNO_3$ (Certified ACS Plus), and muriatic acid (31.45% HCl). Bee Gorge sample BB went through 20% HCl. Bee Gorge samples 96714A & B went through 20% HCl, and some of the spherule layer material in both samples also went through concentrated HCl. JSL sample W94-1Q went through muriatic acid. The following samples went through concentrated HCl: CSL samples 84-1 and X38-2, JSL sample X21-1, and MSL samples U63-1 and V111. CSL samples W85-2, X24-1, and 43-1 went through concentrated HCl, and for each of these samples, pyrite was observed in the initial heavy mineral separates (see below). The 63-125 μm and 125-250 μm heavy mineral separates of sample W85-2, the 63-125 μm heavy mineral separates of sample X24-1, and the HCl-insoluble materials in the 63-125 μm and

125-250 µm size fractions of sample 43-1 went through concentrated $HNO_3$ in order to dissolve the pyrite. The following samples went through concentrated $HNO_3$: CSL sample 42-1A, Carawine context samples X68-1, 104141, and 104175, Bee Gorge context sample 92058, and Monteville context samples T149-1 and II67-1B.

For acid digestion, each subsample was put in a glass beaker (± a stirring magnet) with a few hundred milliliters of acid, and the beaker was put on a hotplate for about four to ten hours per day. Additional acid was added to the beaker as needed. For most subsamples, acid digestion was complete in about two to seven days. The beaker was then removed from the hotplate, topped off with water, and the acid-insoluble material was allowed to settle. The acidic water was decanted using a suction device attached to a sink faucet. The beaker was again filled with water, and the material was allowed to settle. For most samples, the acidic water was diluted with tap water, but distilled water was used to dilute Carawine context sample 104175. For CSL sample 42-1A, dilution and wet sieving (see below) were done using only distilled water. Most samples were acid-free after four to eight dilution and decantation cycles.

Wet sieving. The acid-insoluble residues were wet sieved in conjunction with ultrasonic agitation, typically into the following five size fractions: <38 µm, 38-63 µm, 63-125 µm, 125-250 µm, and >250 µm. The >38 µm size fractions were dried under a heat lamp, and the <38 µm size fraction was dried in the oven. For each size fraction, the acid-insoluble material was weighed on the analytical balance, and it was put in one or more glass vials.

Heavy liquid separation. For JSL sample X21-1 and Bee Gorge samples 96714A & B, the 63-125 µm size fractions went through heavy liquid separation. For the remaining samples, the 63-125 µm and 125-250 µm size fractions went through heavy liquid separation. The separations were done in 500 ml or 1 L separatory funnels using Fisher Scientific laboratory grade 1,1,2,2-

tetrabromoethane ($\rho$ = 2.96 g/cm$^3$). Each separation was allowed to settle overnight. For a given size fraction of a given subsample, one to three separations were done. After each separation, the heavy mineral separate was collected in a Whatman® filter (Catalog # 1001-185) with a pore size of 11 µm. Upon completion of the separations, the light fraction ($\rho$ <2.96 g/cm$^3$) was collected in a filter. The filters were rinsed for several days with acetone to remove as much of the heavy liquid as possible.

Transfer of heavy mineral grains to glass cavity slides. For most of the samples, the heavy mineral grains in the filters were transferred directly to cavity slides. For CSL samples 84-1 and 42-1A, Carawine context sample X68-1, Bee Gorge context sample 92058, MSL sample U63-1, and Monteville context samples T149-1 and II67-1B, secondary iron and/or manganese oxide/oxyhydroxide grains were abundant in the heavy mineral separates, so these separates were generally transferred directly to glass vials. For each of these seven samples, these separates were transferred from the vial(s) to a shallow aluminum pan, and using a binocular microscope and a small wetted brush, the grains in these separates that were not obvious secondary iron and/or manganese oxide/oxyhydroxide grains were handpicked and transferred to cavity slides. For all the samples, the heavy mineral grains in the cavity slides were sorted on the basis of their physical similarities (e.g., habit, color) and aligned in rows.

Analytical techniques. Raman measurements were performed using a Senterra Raman microscope spectrometer (Bruker Optics, Inc., Billerica, Massachusetts) at the University of Delaware. Sample excitation was done using 532 nm (Nd:YAG) and 785 nm (diode) laser sources, in which the nominal power ranged from 2-10 mW and 10-50 mW for the laser sources, respectively. The laser beam was focused on the sample using an MPlan 50× objective lens (Olympus, New York, USA) with a numerical aperture of 0.75, yielding a circular probing area

with a diameter of ~2 µm. Laser exposure times of 2-60 seconds were used with spectral co-averages ranging from two to six. Resulting Raman scattering was detected using a thermoelectrically-cooled charge-coupled device (CCD) operating at a temperature of -65 °C, along with a 1200 grooves/mm grating and a slit aperture of 50 by 1000 µm. Raman spectra of neon and laser/neon internal calibration standards were collected prior to each sample spectrum. The Raman spectra were obtained with a resolution of 3-5 $cm^{-1}$ over the spectral range of ~80-3500 $cm^{-1}$.

Using a binocular microscope and a small wetted brush, grains selected for analysis by micro-Raman spectroscopy were removed from a cavity slide, and they were put in a row on a flat glass microscope slide. This slide was placed on the stage of the Raman microscope. For all the samples, we analyzed ~2532 heavy mineral grains, including 165 grains from the 125-250 µm size fraction. This total does not include grains that were analyzed and found to be either laboratory contaminant particles (e.g., solder and rust) or iron and/or manganese oxide/oxyhydroxide phases and pyrite that we interpret to be secondary phases. One analysis per grain was done for ~90% of the grains. We typically analyzed three or four spots per grain for the grains containing the high-pressure polymorph $TiO_2$-II.

Phase identification was done by comparing our Raman spectra with Raman spectra of standard materials from the open-access Raman spectral database of the RRUFF project (Lafuente et al., 2015; http://rruff.info). The identification of the high-pressure polymorph $TiO_2$-II was done by comparing our Raman spectra with Raman spectra of two samples of synthetic $TiO_2$-II. In Figures 2 and 3, the Raman spectrum labeled "Synthetic $TiO_2$-$II^A$" is from El Goresy et al. (2001, see their figure 2), and the measurement parameters for this spectrum are given in El Goresy et al. (2001). This $TiO_2$-II sample was synthesized (see Linde and De Carli, 1969) by

experimentally shock-loading dry rutile powder at a pressure of 20 GPa (El Goresy et al., 2001). The Raman spectra of the four spherule layer grains in Figure 2, the Raman spectra of the three spots on the grain shown in Figure 3, and the Raman spectrum labeled "Synthetic $TiO_2$-II$^B$" (Figs. 2 and 3) were collected at 532-nm excitation using the same Raman microscope spectrometer. This sample of synthetic $TiO_2$-II was obtained from K. Spektor (Stockholm University), and the sample was synthesized at a pressure of 10 GPa and a temperature of 500 °C from rutile powder using the same (K. Spektor, personal communication, August, 2015) static high-pressure hydrothermal conditions that are given in Spektor et al. (2013). In Figures 2 and 3, the Raman spectrum labeled "Rutile" is from the Raman spectral database of the RRUFF project (Lafuente et al., 2015; http://rruff.info). This Raman spectrum was collected at 532-nm excitation, and the RRUFF identification (ID) number for this Raman spectrum is R050031.3 (depolarized).

Using a binocular microscope with up to 50× magnification, F. C. Smith did grain counts for 22 samples to determine the heavy mineral assemblages. Secondary iron and/or manganese oxide/oxyhydroxide grains and pyrite grains are not included in the heavy mineral assemblages given in Tables DR4-DR7. Most of the heavy mineral grains were identified on the basis of their physical similarities (e.g., habit, color) to those of the grains that were analyzed by micro-Raman spectroscopy. No grain count was done for Bee Gorge context sample 92058 (Table DR6) because the predominant heavy mineral phases, xenotime and monazite, are quite similar in appearance. An approximate relative abundance of the heavy mineral phases in sample 92058 was obtained by micro-Raman analysis of 83 grains from the 63-125 μm size fraction (Table DR6).

Back-scattered electron and secondary electron images were obtained for three $TiO_2$-II-bearing grains in uncoated polished grain mounts using an FEI Quanta 450 FEG scanning electron microscope (SEM) operated at low vacuum and 10-30 kV in conjunction with Oxford AZtec energy dispersive spectroscopy. The $TiO_2$-II-bearing grains were mounted with other grains on circular (diameter = 25.4 mm) glass slides using thin-section epoxy. A few drops of epoxy were put around the periphery of the slide to provide balance during the grinding and polishing steps, and across the center of the slide to hold the grains. Using a binocular microscope, the grains were placed on the slide and a sketch was made of the drops and grains. The mounting medium was allowed to harden overnight. Grinding by hand on a wetted 600 grit paper strip was done until the $TiO_2$-II-bearing grains were slightly exposed as determined by examining the slide using a binocular microscope. The grains were polished by hand on a 6-µm-grit paper strip that was wetted with a solution of water, detergent, and glycerol. A final polish was done by hand using 0.05-µm $Al_2O_3$ powder that was wetted with water.

**SUPPLEMENTARY FIGURES**

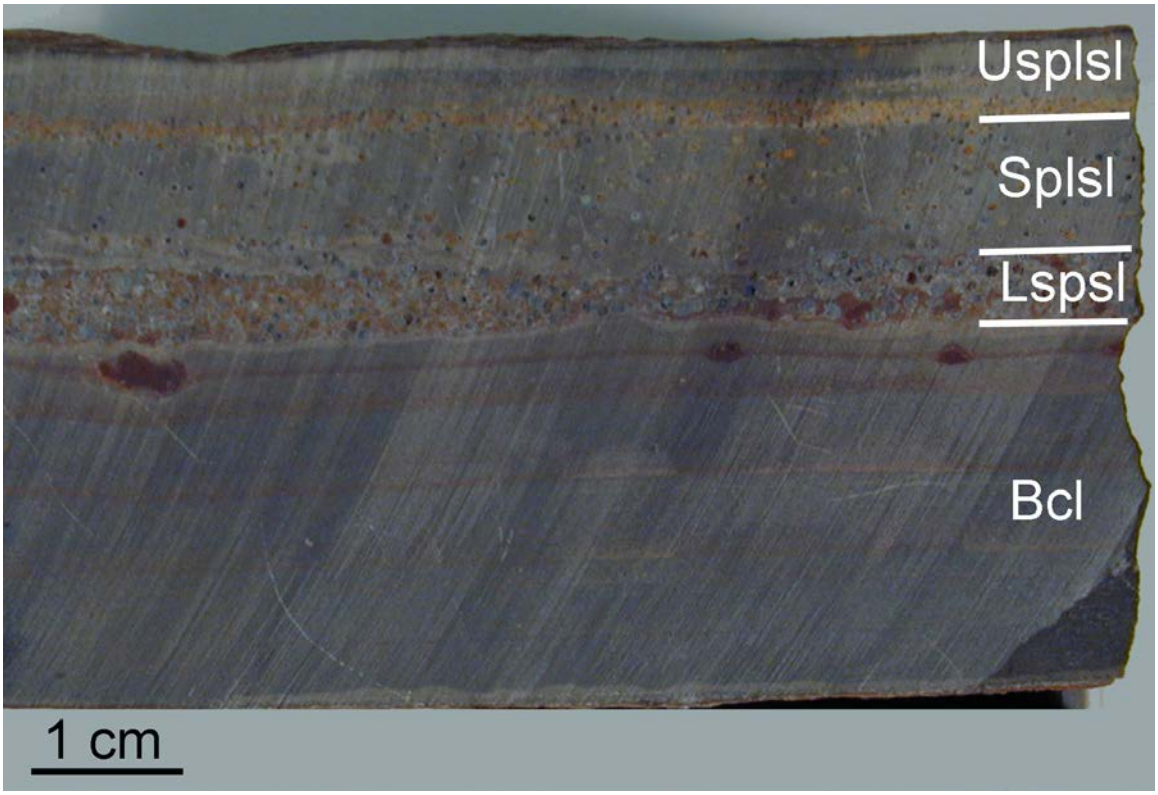


**Figure DR1.** Photograph of a sawn surface of Bee Gorge sample 96714A showing stratigraphic subdivisions. The sample is from the Tom Price site (Fig. 1). The basal carbonate lutite (Bcl) context layer is sharply overlain by the Bee Gorge spherule layer (BGSL). The BGSL consists of the lowermost spherule-rich sublayer (Lspsl) subdivision, the spherule-bearing lutite sublayer (Splsl) subdivision, and the upper spherule/lutite sublayers (Usplsl) subdivision. The white line segments show the boundaries of the subdivisions. The four stratigraphic subdivisions were processed separately (see Methods in Data Repository). For each subdivision, the heavy mineral assemblage is given in Table DR6. $TiO_2$-II-bearing grains were found only in the Usplsl subdivision (Table 1).

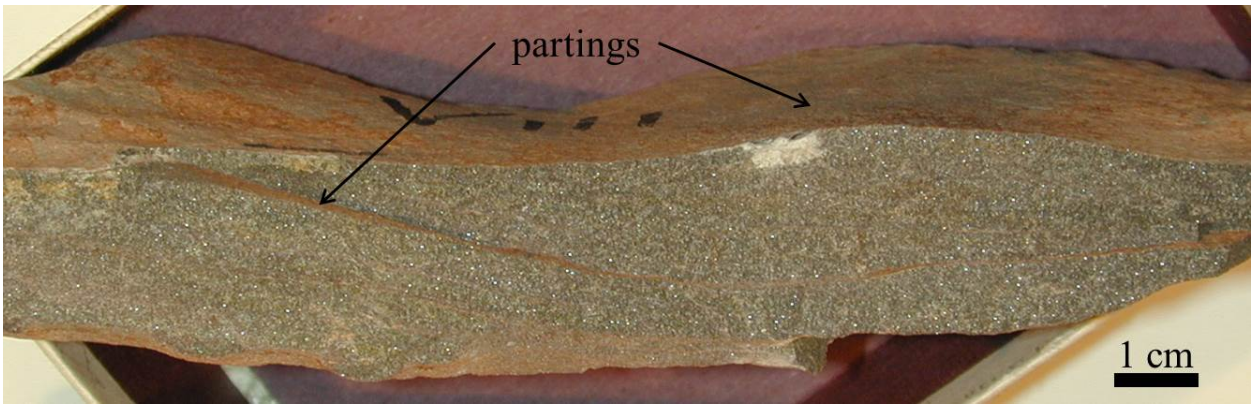


**Figure DR2.** Photograph of Monteville spherule layer (MSL) sample V111. The sample is a fine-to-medium-grained dolarenite from the upper part of the MSL at the Monteville Farm (MF) site (Fig. 1; Table DR3). The sample contains minor fine-grained spherule debris and siliciclastic grains (not visible in photograph). The heavy mineral assemblage of this sample is given in Table DR7. $TiO_2$-II-bearing grains were recovered from this sample (Table 1). The arrows denote partings that are coated by iron oxide/oxyhydroxide material. The partings follow cross-stratification that may be hummocky (Simonson et al., 1999).

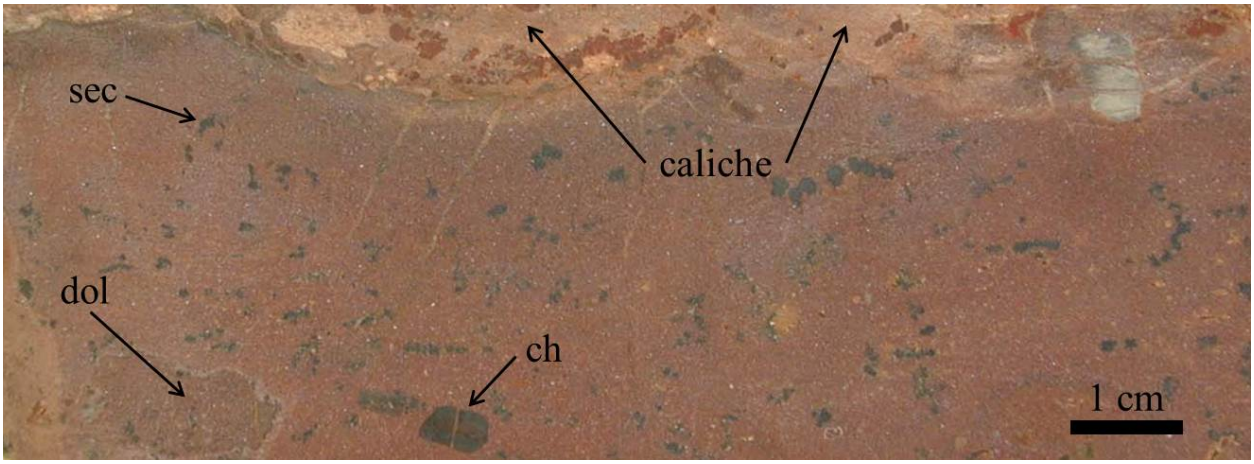


**Figure DR3.** Photograph of a sawn surface of Carawine spherule layer (CSL) sample X38-2. The sample is a dolomixtite from the upper part of the upper unit (Hassler et al., 2005) of the CSL (Table DR1) at the Tarra Tarra Turnoff (TTT) site (Fig. 1). Arrows denote caliche, a small chert (ch) fragment, an oversized dolomite (dol) clast, and dark, fine-grained secondary (sec) material that probably represents oxidized pyrite bodies. Spherules and irregular melt particles (Hassler et al., 2005) are sparse in the sample. The heavy mineral assemblage of this sample is given in Table DR4. $TiO_2$-II-bearing grains were recovered from this sample (Table 1).

## SUPPLEMENTARY TABLES

**Table DR1. Location and lithology for Carawine Dolomite and Jeerinah Formation samples**

| Sample number | Informal site name | Latitude, longitude | Position within or with respect to the spherule layer | Lithology |
|---|---|---|---|---|
| | | **Carawine spherule layer samples** | | |
| X38-2 | Tarra Tarra Turnoff (TTT) | 21°48′S, 121°13′30″E | Sandy upper part of dolomixtite of upper unit | Dolomixtite |
| 42-1A | Ripon Hills south (RS) | 21°18′S, 120°46′30″E | In upper unit within 75 cm of top of layer | Sandy dolomixtite |
| 43-1 | Ripon Hills south (RS) | 21°18′S, 120°46′30″E | Finer zone near top of lower unit | Dolomixtite |
| X24-1 | Ripon Hills (RH) | 21°20′05.1″S, 120°45′32.8″E | Lower unit | Dolomixtite |
| 84-1 | Ripon Hills south (RS) | 21°18′S, 120°46′30″E | In lower unit within 20 cm of base of layer | Calcareous dolomixtite |
| W85-2 | Ripon Hills (RH) | 21°18′39.7″S, 120°46′21.4″E | Float from lower unit of layer | Dolomixtite |
| | | **Carawine context samples** | | |
| 104175 | Ripon Hills south (RS) | 21°18′S, 120°46′30″E | ~20 m above | Laminated dololutite |
| 104141 | Ripon Hills southeast (RE) | 21°18′30″S, 120°52′E | ~5 m below | Laminated dololutite |
| X68-1 | Tarra Tarra Turnoff (TTT) | 21°48′S, 121°13′30″E | 10-20 m below | Laminated dololutite |
| | | **Jeerinah spherule layer samples** | | |
| X21-1 & W94-1Q | Hesta Siding | 22°11.8′S, 119°1.6′E* | Two pieces of float from the basal thin-bedded zone | Ferruginous rocks rich in melt particles† and large rip-up clasts with fine-grained carbonate-rich matrices |

*Notes*: At the Tarra Tarra Turnoff site and the sites in the Ripon Hills, the Carawine spherule layer is subdivided into three stratigraphic units (Hassler et al., 2005). At the Hesta site, the Jeerinah spherule layer is subdivided into three stratigraphic zones (units) (Hassler et al., 2005).
*The latitude and longitude values for the Hesta site are from Hassler et al. (2005).
†The term “melt particles” refers to both spherules and irregular melt particles (see Hassler et al., 2005).

**Table DR2. Location and lithology for Bee Gorge Member (Wittenoom Formation) samples**

| Sample number | Informal site name | Latitude, longitude* | Lithology/stratigraphy |
|---|---|---|---|
| **Samples that consist of the Bee Gorge spherule layer and a context layer** | | | |
| 96714A & 96714B[†] | Tom Price (TP) water tank | 22°45′S, 117°45′E | Basal carbonate lutite context layer sharply overlain by a spherule-bearing dolomitic lutite layer |
| **Sample that consists of the Bee Gorge spherule layer and two context layers** | | | |
| BB[§] | Bacon Bore (BB) | 21°58′S, 117°36′E | Spherule-rich layer with a carbonate lutite matrix sandwiched between two carbonate lutite context layers |
| **Bee Gorge context sample** | | | |
| 92058 | Wittenoom Gorge (WG) (Cathedral Pool) | 22°19′S, 118°20′E | Fine-grained calcarenite ~1 m stratigraphically above the Bee Gorge spherule layer |

*The latitude and longitude values for all samples are from Simonson et al. (1993).
[†]Samples 96714A & B are two mirror-image slabs from the same hand sample that encompass the same stratigraphic interval. For the two samples, the basal carbonate lutite context layer is ~2.3-2.4 cm thick, and the Bee Gorge spherule layer is ~1.3-2.1 cm thick (see e.g., Fig. DR1).
[§]For sample BB, the spherule layer is ~8-14 mm thick, and each of the context layers is ≤11 mm thick. The direction of stratigraphic "up" in the sample is unknown.

**Table DR3. Location and lithology for Monteville Formation samples**

| Sample number | Location | Latitude, longitude* | Position within or with respect to the spherule layer | Lithology |
|---|---|---|---|---|
| **Monteville spherule layer samples** | | | | |
| V111 | Monteville Farm | 28°36′S, 23°58.5′E | Upper part | Fine-to-medium dolarenite |
| U63-1 | Monteville Farm | 28°36′S, 23°58.5′E | Lower part | Dolarenite rich in spherules with large rip-up clasts of dololutite, shale, and pyrite |
| **Monteville context samples** | | | | |
| II67-1B | Monteville Farm | 28°36′S, 23°58.5′E | ~20 cm above | Dololutite with probable microbial structures |
| T149-1 | Monteville Farm | 28°36′S, 23°58.5′E | ~1 m below | Massive calcilutite |

**Table DR4. Heavy mineral assemblages for Carawine spherule layer and context samples**

| Sample number | Weight (g)* | Number of heavy mineral grains | Number of heavy mineral grains/kg | Heavy mineral phases (63-125 µm size fraction) | | |
|---|---|---|---|---|---|---|
| | | | | Major (>10%)[†] | Minor (1-10%)[†] | Trace (<1%) |
| **Carawine spherule layer samples** | | | | | | |
| **X38-2[§]** | 229.4 | 1716 | 7480 | Ant, Rt (n = 233), Zrn | Crspl, Tur, Unid | Ang, Brk, Czo/Ep |
| 42-1A | 557.5 | 599 | 1074 | Ant | Zrn, Rt (n = 28), Unid, Crspl | Tur |
| 43-1 | 5151.7 | 778 | 151 | Ant | Unid, Zrn, Rt (n = 11) | Act, Brk, Crspl |
| X24-1 | 1472.6 | 556 | 378 | Ant | Zrn, Rt (n = 15), Czo/Ep, Unid, Tur | Act, Amp, Cpx, Crspl |
| 84-1 | 268.1 | 703 | 2622 | Ant | Czo/Ep, Unid, Rt (n = 24), Zrn | Act, Ang, Crspl, Opx, Tur |
| W85-2 | 649.4 | 178 | 274 | Ant, Unid | Act, Ang, Alm, Zrn | Amp, Crspl, Czo/Ep, Rt (n = 1), Tur |
| **Carawine context samples** | | | | | | |
| 104175 | 235.4 | 2 | 8 | Unid | - | - |
| 104141 | 357.2 | 89 | 249 | Ant, Crspl | Zrn, Tur, Rt (n = 2) | - |
| X68-1 | 604.7 | 9 | 15 | Ant, Rt (n = 3), Tur | - | - |

*Notes*: n = the number of rutile grains in the 63-125 µm size fraction.
Mineral abbreviations for Tables DR4-DR7: Act = actinolite; Alm = almandine; Amp = amphibole; Ang = anglesite; Ant = anatase; Brk = brookite; Brt = barite; Chl = chlorite; Cpx = clinopyroxene; Crspl = chrome spinel; Czo = clinozoisite; Ep = epidote; Hem = hematite; Ilm = ilmenite; Mnz = monazite; Opx = orthopyroxene; Rt = rutile; Sil = sillimanite; Tur = tourmaline; Unid = unidentified; Xtm = xenotime; Zrn = zircon.
*The number of decimal places for the weight values is explained in Methods in the Data Repository.
[†]The abundance of a phase is greater than or equal to that of the following phase.
[§]A sample in boldface has some rutile grains that contain the high-pressure polymorph $TiO_2$-II.

**Table DR5. Heavy mineral assemblages for Jeerinah spherule layer samples**

| Sample number | Weight (g)* | Number of heavy mineral grains | Number of heavy mineral grains/kg | Heavy mineral phases (63-125 µm size fraction) | | |
|---|---|---|---|---|---|---|
| | | | | Major (>10%) | Minor (1-10%)[†] | Trace (<1%) |
| **X21-1**[§] | 265.52 | 3639 | 13705 | Ant | Rt (n = 196), Zrn | Act, Ang, Brk, Brt, Cpx, Crspl, Hem, Tur, Unid |
| W94-1Q | 38.73 | 769 | 19855 | Ant | Rt (n = 20) | Crspl, Ilm, Tur, Zrn |

*Notes*: n = the number of rutile grains in the 63-125 µm size fraction.
Mineral abbreviations are given in the footnotes for Table DR4.
*The number of decimal places for the weight values is explained in Methods in the Data Repository.
[†]The abundance of a phase is greater than or equal to that of the following phase.
[§]A sample in boldface has some rutile grains that contain the high-pressure polymorph $TiO_2$-II.

**Table DR6. Heavy mineral assemblages for Bee Gorge Member (Wittenoom Formation) samples**

| Sample number (layer or sublayer(s)) | Weight (g)* | Number of heavy mineral grains | Number of heavy mineral grains/kg | Heavy mineral phases (63-125 µm size fraction) | | |
|---|---|---|---|---|---|---|
| | | | | Major (>10%)[†] | Minor (1-10%)[†] | Trace (<1%) |
| **Bee Gorge spherule layer samples (layer/sublayer(s))** | | | | | | |
| **96714A (U)[§]** | 17.19 | 78 | 4538 | Rt (n = 62), Ant | Ang | - |
| 96714A (S) | 10.36 | 4 | 386 | Ant, Ang | - | - |
| 96714A (L) | 15.92 | 519 | 32601 | Rt (n = 515) | - | Alm, Ant |
| **96714B (U)[§]** | 14.22 | 53 | 3726 | Rt (n = 28), Xtm, Ant | Mnz, Unid | - |
| 96714B (S) | 18.58 | 26 | 1399 | Ant, Rt (n = 10) | Act | - |
| 96714B (L) | 13.82 | 439 | 31771 | Rt (n = 434) | Ant | Mnz |
| BB (sl) | 31.24 | 71 | 2273 | Ant, Rt (n = 19) | Tur, Zrn, Act, Mnz, Unid, Crspl, Czo/Ep | - |
| **Bee Gorge context samples (layer)** | | | | | | |
| 96714A (Bcl) | 82.26 | 41 | 498 | Ant | Rt (n = 4) | - |
| 96714B (Bcl) | 52.76 | 13 | 246 | Ant | Sil | - |
| BB (#2) | 14.89 | 33 | 2216 | Rt (n = 14), Zrn, Ant, Tur | Unid, Ang, Crspl, Czo/Ep | - |
| BB (#1) | 5.40 | 10 | 1851 | Rt (n = 3), Tur, Unid | Ant, Czo/Ep, Zrn | - |
| 92058 | 236.3 | 83[#] | - | Xtm, Mnz[#] | Ant, Rt (n = 3)[#] | - |

*Notes*: Bcl = Basal carbonate lutite layer; L = Lowermost spherule-rich sublayer (Lspsl); n = the number of rutile grains in the 63-125 µm size fraction; S = Spherule-bearing lutite sublayer (Splsl); sl = spherule layer; U = Upper spherule/lutite sublayers (Usplsl).
Mineral abbreviations are given in the footnotes for Table DR4.
*The number of decimal places for the weight values is explained in Methods in the Data Repository.
[†]The abundance of a phase is greater than or equal to that of the following phase.
[§]Sublayers in boldface have some rutile grains that contain the high-pressure polymorph $TiO_2$-II.
[#]An approximate relative abundance of heavy minerals for sample 92058 is based on the analysis of 83 grains (see Methods in the Data Repository).

**Table DR7. Heavy mineral assemblages for Monteville spherule layer and context samples**

| Sample number | Weight (g)* | Number of heavy mineral grains | Number of heavy mineral grains/kg | Heavy mineral phases (63-125 µm size fraction) | | |
|---|---|---|---|---|---|---|
| | | | | Major (>10%)[†] | Minor (1-10%)[†] | Trace (<1%) |
| **Monteville spherule layer samples** | | | | | | |
| **V111[§]** | 219.9 | 2789 | 12683 | Ant, Mnz, Rt (n = 373) | Zrn, Tur | Act, Ang, Chl, Cpx, Crspl, Unid |
| U63-1 | 593.2 | 1231 | 2075 | Ant, Mnz | Rt (n = 18), Unid | Chl, Tur |
| **Monteville context samples** | | | | | | |
| II67-1B | 616.7 | 22 | 36 | Ant, Crspl | Rt (n = 1) | - |
| T149-1 | 214.3 | 169 | 789 | Mnz, Chl | Ant | - |

*Notes*: n = the number of rutile grains in the 63-125 µm size fraction.
Mineral abbreviations are given in the footnotes for Table DR4.
*The number of decimal places for the weight values is explained in Methods in the Data Repository.
[†]The abundance of a phase is greater than or equal to that of the following phase.
[§]A sample in boldface has some rutile grains that contain the high-pressure polymorph $TiO_2$-II.

## REFERENCES CITED

El Goresy, A., Chen, M., Gillet, P., Dubrovinsky, L., Graup, G., and Ahuja, R., 2001, A natural shock-induced dense polymorph of rutile with α-$PbO_2$ structure in the suevite from the Ries crater in Germany: Earth and Planetary Science Letters, v. 192, p. 485-495, doi: 10.1016/S0012-821X(01)00480-0.

Hassler, S.W., Simonson, B.M., Sumner, D.Y., and Murphy, M., 2005, Neoarchaean impact spherule layers in the Fortescue and Hamersley Groups, Western Australia: stratigraphic and depositional implications of re-correlation: Australian Journal of Earth Sciences, v. 52, p. 759-771, doi: 10.1080/08120090500170369.

Lafuente, B., Downs, R.T., Yang, H., and Stone, N., 2015, The power of databases: The RRUFF project, *in* Armbruster, T., and Danisi, R.M., eds., Highlights in Mineralogical Crystallography: Berlin, W. De Gruyter, p. 1-30.

Linde, R.K., and De Carli, P.S., 1969, Polymorphic behavior of titania under dynamic loading: The Journal of Chemical Physics, v. 50, p. 319-325, doi: 10.1063/1.1670796.

Simonson, B.M., Hassler, S.W., and Schubel, K.A., 1993, Lithology and proposed revisions in stratigraphic nomenclature of the Wittenoom Formation (Dolomite) and overlying formations, Hamersley Group, Western Australia: Geological Survey of Western Australia Report 34, Professional Papers, p. 65-79.

Simonson, B.M., Hassler, S.W., and Beukes, N.J., 1999, Late Archean impact spherule layer in South Africa that may correlate with a Western Australian layer, *in* Dressler, B.O., and Sharpton, V.L., eds., Large meteorite impacts and planetary evolution II: Geological Society of America Special Paper 339, p. 249-262.

Spektor, K., Tran, D.T., Leinenweber, K., and Häussermann, U., 2013, Transformation of rutile to $TiO_2$-II in a high pressure hydrothermal environment: Journal of Solid State Chemistry, v. 206, p. 209-216, doi: 10.1016/j.jssc.2013.08.018.